Influence of particle shape on shear stress in granular media

Emilien Azéma[1], Farhang Radjaï[1], Robert Peyroux[1] and Gilles Saussine[2]

[1] LMGC, CNRS - Université Montpellier II, Place Eugène Bataillon, 34095 Montpellier cedex 05, France. azema@lmgc.univ-montp2.fr
[2] Innovation and Research Departement of SNCF, 45 rue de Londres, 75379 PARIS Cedex 08 gilles.saussine@sncf.fr

We analyze the contact and force networks in a dense confined packing of pentagonal particles simulated by means of the contact dynamics method. The particle shape effect is evidenced by comparing the data from pentagon packing and from a packing with identical characteristics except for the circular shape of the particles. A surprising observation is that the pentagon packing develops a lower structural anisotropy than the disk packing. We show in this work that this weakness is compensated by a higher force anisotropy that leads to enhanced shear strength of the pentagon packing. With the polygonal shape of the particles, the strong force chains are mostly composed of edge-to-edge contacts with a marked zig-zag aspect.

1 Introduction

The microstructure of granular materials is generically anisotropic in two respects: 1) The contact normal directions are not random; 2) The force average as a function of contact normal direction is not uniform. The corresponding fabric and force anisotropies in shear are responsible for mechanical strength at the scale of the packing [11, 12, 13, 10]. The shear stress is fully transmitted via a "strong" contact network, materialized by force "chains" and the stability is ensured by the antagonist role of "weak" contacts which prop strong force chains[10, 14]. These features have, however, been for the most part investigated in the case of granular media composed of isometric (circular or spheric) particles.

In this paper, we consider one of the simplest possible shapes, namely regular pentagons. Among regular polygons, the pentagon has the lowest number of sides, corresponding to the least roundedness in this category, without the pathological space-filling properties of triangles and squares. We seek to isolate the effect of edge-to-edge contacts on shear stress and force transmission by comparing the data with a packing of circular particles that, apart from

the particle shape, is fully identical (preparation, friction coefficients, particle size distribution) to the pentagon packing. Both packings are subjected to biaxial compression simulated by means of the contact dynamics method. The presence of edge-to-edge contacts affects both quantitatively and qualitatively the microstructure and the overall behavior during shear. These contacts do not transmit torques, but they are able to accommodate force lines that are usually unsustainable in packings of disks.

2 Numerical procedures

The simulations were carried out by means of the contact dynamics (CD) method with pentagonal particles. The CD method is based on implicit time integration of the equations of motion and a nonsmooth formulation of mutual exclusion and dry friction between particles [15, 16, 17]. This method requires no elastic repulsive potential and no smoothing of the Coulomb friction law for the determination of forces. For this reason, the simulations can be performed with large time steps compared to molecular dynamics simulations. We used LMGC90 which is a multipurpose software developed in our laboratory, capable of modeling a collection of deformable or undeformable particles of various shapes by different algorithms [18].

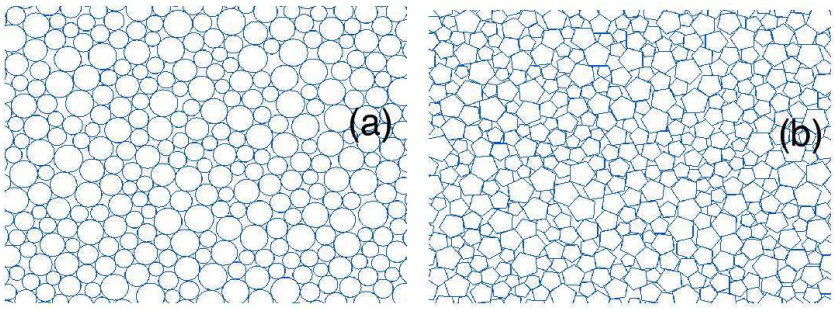

Fig. 1. Snapshots of a portion of the samples S2 (a) and S1 (b) composed of circular and pentagonal particles, respectively.

We generated two numerical samples. The first sample S1, is composed of 14400 regular pentagons of three different diameters: 50% of diameter 2.5 cm, 34% of diameter 3.75 cm and 16% of diameter 5 cm. The second sample S2, is composed of 10000 discs with the same polydispersity. Both samples were prepared according to the same protocol. The gravity was set to zero in order to avoid force gradients in the samples. The coefficient of friction was set to 0.4 between grains and to 0 with the walls. At equilibrium, both numerical samples were in isotropic stress state. The solid fraction was $\phi_0 = 0.80$ for S1

and $\phi_0 = 0.82$ for S2. The aspect ratio was $h/l \approx 2$, where h and l are the height and width of the sample, respectively. Figure 1 displays snapshots of the two packings at the end of isotropic compaction.

The isotropic samples were subjected to vertical compression by downward displacement of the top wall at a constant velocity of 1 cm/s for a constant confining stress σ_0 acting on the lateral walls. Since we are interested in quasistatic behavior, the shear rate should be such that the kinetic energy supplied by shearing is negligible compared to the static pressure. This can be formulated in terms of an "inertia parameter" I defined by [19]

$$I = \dot{\varepsilon}\sqrt{\frac{m}{p}}, \tag{1}$$

where $\dot{\varepsilon} = \dot{y}/y$ is the strain rate, m is the total mass, and p is the average pressure. The quasistatic limit is characterized by the condition $I \ll 1$. In our biaxial simulations, I was below 10^{-3}.

3 Shear stress

In this section, we compare the stress-strain behavior between the packings of polygons (sample S1) and disks (sample S2). For the calculation of the stress tensor, we consider the "tensorial moment" $\boldsymbol{M}^i$ of each particle i defined by [20, 14]:

$$M^i_{\alpha\beta} = \sum_{c\in i} f^c_\alpha r^c_\beta, \tag{2}$$

where f^c_α is the α component of the force exerted on particle i at the contact c, r^c_β is the β component of the position vector of the same contact c, and the summation is runs over all contacts c of neighboring particles with the particle i (noted briefly by $c \in i$). It can be shown that the tensorial moment of a collection of rigid particles is the sum of the tensorial moments of individual particles. The stress tensor $\boldsymbol{\sigma}$ for a packing of volume V is simply given by [20, 14]:

$$\boldsymbol{\sigma} = \frac{1}{V}\sum_{i\in V}\boldsymbol{M}^i = \frac{1}{V}\sum_{c\in V} f^c_\alpha \ell^c_\beta, \tag{3}$$

where $\boldsymbol{\ell}^c$ is the intercenter vector joining the centers of the two touching particles at the contact c. We extract the mean stress $p = (\sigma_1 + \sigma_2)/2$, and the stress deviator $q = (\sigma_1 - \sigma_2)/2$, where σ_1 and σ_2 are the principal stresses. The major principal direction during vertical compression is vertical, we then define the volumetric strain by :

$$\varepsilon_p = \int_{V_0}^{V} \frac{dV'}{V'} = \ln\left(1 + \frac{\Delta V}{V_0}\right), \tag{4}$$

where V_0 is the initial volume and $\Delta V = V - V_0$ is the cumulative volume change.

Figure 2 shows the normalized shear stress q/p for the samples S1 and S2 as a function of shear strain $\varepsilon_q \equiv \varepsilon_1 - \varepsilon_2$. For S2, we observe a hardening behavior followed by (slight) softening and a stress plateau corresponding to the residual state of soil mechanics [21]. For S1, we observe no marked stress peak. The residual stress is higher for polygons ($\simeq 0.35$) than for disks ($\simeq 0.28$). The higher level of q/p for the polygon packing reflects the organization of the microstructure and the features of force transmission that we analyze in more detail below.

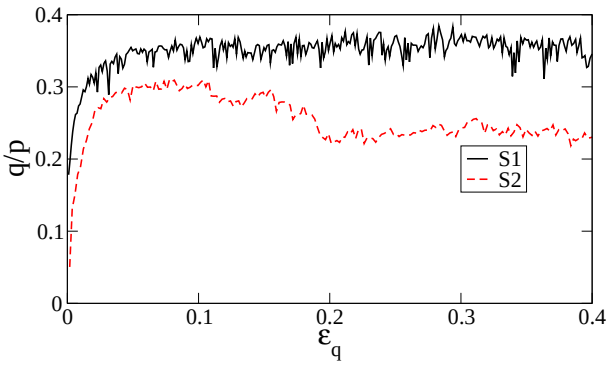

Fig. 2. Normalized shear stress q/p as a function of cumulative shear strain ε_q for the samples S1 and S2.

4 Fabric anisotropy

The shear strength of dry granular materials is generally attributed to the buildup of an anisotropic structure during shear due to friction between the particles and as a result of steric effects depending on particle shape [22, 23, 24].

The probability density function $P_\theta(\theta)$, where θ is the orientation of the contact normal $\boldsymbol{n}$, provides the basic orientational statistical information about the granular the fabric. It is π-periodic in the absence of an intrinsic polarity for $\boldsymbol{n}$. Most lowest-order information is generally given by the second moment of P_θ, called *fabric tensor* [25]:

$$F_{\alpha\beta} = \frac{1}{\pi}\int_0^\pi n_\alpha(\theta) n_\beta(\theta) P_\theta(\theta) d\theta \equiv \frac{1}{N_c}\sum_{c\in V} n_\alpha^c n_\beta^c, \tag{5}$$

where α and β design the components in a reference frame and N_c is the total number of contacts in the control volume V. By definition, $tr(\boldsymbol{F}) = 1$. The anisotropy of the contact network is given the difference between the principal values F_1 and F_2. We define the fabric anisotropy a by

$$a = 2(F_1 - F_2). \tag{6}$$

Figure 3 displays a polar representation of $P_\theta(\theta)$ for the samples S1 and S2 at $\varepsilon_q = 0.3$. We observe a nearly isotropic distribution for the pentagon packing in spite of shearing whereas the disk packing is markedly anisotropic. This is a surprising observation in view of the higher shear strength of the pentagon packing.

The evolution of a is shown in Fig. 4 as a function of ε_q for S1 and S2. The anisotropy stays quite weak in the pentagon packing whereas the disk packing is marked by a much larger anisotropy, increasing to $\simeq 0.3$ and then relaxing to a slightly lower value in the residual state. The low anisotropy of the pentagon packing results from a particular organization of the force network in correlation with the orientations of edge-to-edge and vertex-to-edge contacts in the packing [26]. This leads us to consider the contributions of force and texture anisotropies to average shear stresses.

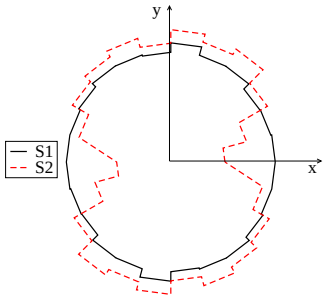

Fig. 3. Polar representation of the probability density function P_θ of the contact normal directions θ for the samples S1 and S2 in the residual state.

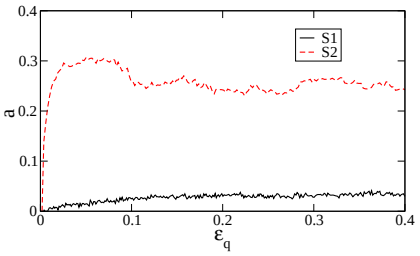

Fig. 4. Evolution of the anisotropy a with cumulative shear strain ε_q for the samples S1 and S2.

5 Force anisotropy

The angular distribution of contact forces in a granular packing can be represented by the average force $\langle \boldsymbol{f} \rangle(\boldsymbol{n})$ as a function of the contact normal direction $\boldsymbol{n}$. We distinguish the average normal force $\langle f_n \rangle(\theta)$ from the average tangential force $\langle f_t \rangle(\theta)$. As $P(\theta)$, these two functions can be represented by their Fourier expansions truncated beyond the second term [11, 12, 13, 10]:

$$\begin{cases} \langle f_n \rangle(\theta) = \langle f \rangle \{1 + a_n \cos 2(\theta - \theta_n)\} \\ \langle f_t \rangle(\theta) = \langle f \rangle a_t \sin 2(\theta - \theta_t) \end{cases} \tag{7}$$

where $\langle f \rangle$ is the average force, a_n and a_t represent the anisotropies of the normal and tangential forces, respectively, and θ_n and θ_t are their privileged directions. It is convenient to estimate the anisotropies from the following "force tensors":

$$\begin{cases} H^{(n)}_{\alpha\beta} = \int_0^{\pi} \langle f_n \rangle(\theta) n_\alpha n_\beta d\theta, \\ H^{(t)}_{\alpha\beta} = \int_0^{\pi} \langle f_t \rangle(\theta) n_\alpha t_\beta d\theta. \end{cases} \tag{8}$$

Then, we have $tr(\boldsymbol{H}^{(n)}) = \langle f \rangle$, and

$$\begin{cases} a_n = 2\frac{H^{(n)}_1 - H^{(n)}_2}{H^{(n)}_1 + H^{(n)}_2}, \\ a_t = 2\frac{H^{(t)}_1 - H^{(t)}_2}{H^{(n)}_1 + H^{(n)}_2}, \end{cases} \tag{9}$$

where the subscripts 1 and 2 refer to the principal values of the tensors.

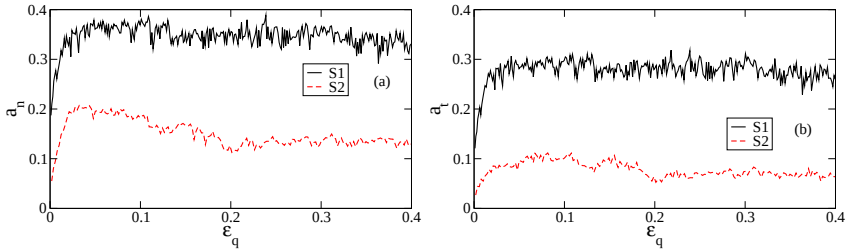

Fig. 5. Evolution of force anisotropies a_n (a) and a_t (b) as a function of cumulative shear strain ε_q in samples S1 and S2.

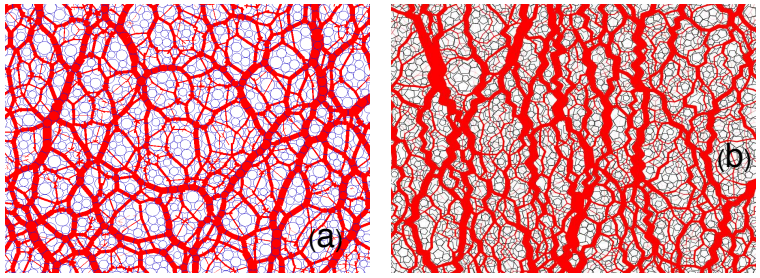

Fig. 6. Snapshots of normal forces in samples S2 (a) and S1 (b). Line thickness is proportional to the normal force.

Figure 5 shows the evolution of a_n and a_t with ε_q in samples S1 and S2. We see that, in contrast to fabric anisotropies (Fig. 4), the force anisotropies in the

pentagon packing remain always above those in the disk packing. This means that the aptitude of the pentagon packing to develop large force anisotropy and strong force chains is not solely dependent on the global fabric anisotropy of the system. Indeed, due to the geometry of the pentagons, i.e. the absence of parallel sides, the strong force chains are mostly of zig-zag shape, as observed in Fig. 6, and the stability of such structures requires strong activation of tangential forces. This explains, in turn, the large value of a_t for pentagons, very close to a_n, whereas in the disk packing a_t is nearly half of a_n.

The anisotropies a, a_n and a_t are interesting descriptors of granular microstructure and force transmission as they underlie the shear stress. Indeed, it can be shown that the general expression of the stress tensor Eq. (3) under some approximations leads to the following simple relation [13, 24]:

$$\frac{q}{p} \simeq \frac{1}{2}(a + a_n + a_t), \tag{10}$$

where the cross products $a_n a$ and $a_t a$ between the anisotropies have been neglected compared to the anisotropies, and it has been assumed that the stress tensor is coaxial with the fabric tensor Eq. (5) and the force tensors Eq. (8). Fig. 7 shows that Eq. (10) holds quite well both for pentagons and disks. This equation provides an amazingly good estimate of the shear stress from the anisotropies under monotonic shearing.

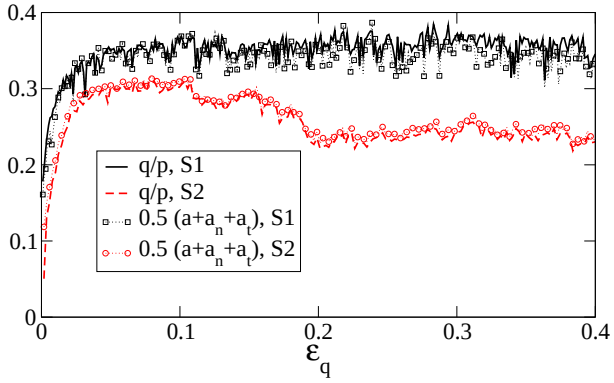

Fig. 7. Evolution of the normalized shear stress q/p for the samples S1 and S2 with ε_q together with the corresponding predictions from its expression as a function of fabric and force anisotropies Eq. (10).

A remarkable consequence of Eq. (10) is to reveal the distinct origins of shear stress in pentagon and disk packings. The fabric anisotropy provides a major contribution to shear stress in the disk packing (Fig. 4) whereas the force anisotropies are more important for shear stress in the pentagon packing (Fig. 5). In this way, in spite of the weak fabric anisotropy a, the larger force

anisotropies a_n and a_t allow the pentagon packing to reach higher levels of q/p compared to the disk packing.

6 Conclusion

The objective of this paper was to isolate the effect of particle shape on shear strength in granular media by comparing two similar packings with different particle shapes: pentagons vs. disks. We observed enhanced shear strength and force inhomogeneity in the pentagon packing. But, unexpectedly, the pentagon packing was found to develop a lower structural (fabric) anisotropy compared to the disk packing under shear. This low fabric anisotropy, however, does not prevent the pentagon packing from building up a strong force anisotropy that underlies its enhanced shear strength compared to the disk packing.

This finding is interesting as it shows that the force anisotropy in a granular material depends on the particle shapes. This mechanism may be the predominant source of strength for "facetted" particles that can give rise edge-to-edge (in 2D) contacts allowing for strong force localization along such contacts in the packing. Since the fabric anisotropy is low in a pentagon packing, the role of force anisotropy and thus the local equilibrium structures are important with respect to its overall strength properties. With pentagon packings, we were able to demonstrate the nontrivial phenomenology resulting from the specific shape of particles as compared to a disk packing. We found a similar behaviour for other regular polygons (hexagons and higher number of sides) as well as polyhedral particles in three dimensions.

References

1. C.-h. Liu, S. R. Nagel, D. A. Schecter, S. N. Coppersmith, S. Majumdar, O. Narayan, and T. A. Witten. Force fluctuations in bead packs. *Science*, 269:513, 1995.
2. F. Radjai, M. Jean, J.J. Moreau, and S. Roux. Force distributions in dense two dimensional granular systems. *Phys. Rev. Letter*, 77:274–277, 1996.
3. S. N. Coppersmith, C.-h. Liu, S. Majumdar, O. Narayan, and T. A. Witten. Model for force fluctuations in bead packs. *Phys. Rev. E*, 53(5):4673–4685, 1996.
4. D. M. Mueth, H. M. Jaeger, and S. R. Nagel. Force distribution in a granular medium. *Phys. Rev. E.*, 57(3):3164–3169, 1998.
5. G. Lovol, K. Maloy, and E. Flekkoy. Force measurments on static granular materials. *Phys. Rev. E*, 60:5872–5878, 1999.
6. S. G. Bardenhagen, J. U. Brackbill, and D. Sulsky. Numerical study of stress distribution in sheared granular material in two dimensions. *Phys. Rev. E*, 62:3882–3890, 2000.
7. S. J. Antony. Evolution of force distribution in three-dimensional granular media. *Phys Rev E*, 63:011302, 2001.

8. T. S. Majmudar and R. P. Behringer. Contact force measurements and stress-induced anisotropy in granular materials. *Nature*, 435:1079–1082, 2005.
9. L. E. Silbert, G. S. Grest, and J. W. Landry. Statistics of the contact network in frictional and frictionless granular packings. *Phys. Rev. E*, 66:1–9, 2002.
10. F. Radjai, D. E. Wolf, M. Jean, and J.J. Moreau. Bimodal character of stress transmission in granular packings. *Phys. Rev. Letter*, 80:61–64, 1998.
11. N. P. Kruyt and L. Rothenburg. Micromechanical definition of strain tensor for granular materials. *ASME Journal of Applied Mechanics*, 118:706–711, 1996.
12. R. J. Bathurst and L. Rothenburg. Micromechanical aspects of isotropic granular assemblies with linear contact interactions. *J. Appl. Mech.*, 55:17, 1988.
13. L. Rothenburg and R. J. Bathurst. Analytical study of induced anisotropy in idealized granular materials. *Geotechnique*, 39:601–614, 1989.
14. L. Staron and F. Radjai. Friction versus texture at the approach of a granular avalanche. *Phys. Rev. E*, 72:1–5, 2005.
15. M. Jean. The non smooth contact dynamics method. *Computer Methods in Applied Mechanic and Engineering*, 177:235–257, 1999.
16. M. Jean and J. J. Moreau. Unilaterality and dry friction in the dynamics of rigid body collections. In *Proceedings of Contact Mechanics International Symposium*, pages 31–48, Lausanne, Switzerland, 1992. Presses Polytechniques et Universitaires Romandes.
17. J.J. Moreau. Some numerical methods in multibody dynamics : application to granular. *Eur. J. Mech. A/Solids*, 13:93–114, 1994.
18. F. Dubois and M. Jean. Lmgc90 une plateforme de développement dédiée à la modélisation des problèmes d'intéraction. In *Actes du sixième colloque national en calcul des structures - CSMA-AFM-LMS* -, volume 1, pages 111–118, 2003.
19. GDR-MiDi. On dense granular flows. *Eur. Phys. J. E*, 14:341–365, 2004.
20. J. J. Moreau. Numerical investigation of shear zones in granular materials. In D. E. Wolf and P. Grassberger, editors, *Friction, Arching, Contact Dynamics*, pages 233–247, Singapore, 1997. World Scientific.
21. J.K. Mitchell and K. Soga. *Fundamentals of Soil Behavior*. Wiley, NY, 2005.
22. M. Oda, J. Koshini, and S. Nemat-Nasser. Some experimentally based fundamental results on the mechanical behavior of granular materials. *Geotechnique*, 30:479–495, 1980.
23. B. Cambou. From global to local variables in granular materials. In C. Thornton, editor, *Powders and Grains 93*, pages 73–86, Amsterdam, 1993. A. A. Balkema.
24. F. Radjai, H. Troadec, and S. Roux. Key features of granular plasticity. In S.J. Antony, W. Hoyle, and Y. Ding, editors, *Granular Materials: Fundamentals and Applications*, pages 157–184, Cambridge, 2004. RS.C.
25. M. Satake. Fabric tensor in granular materials. In P. A. Vermeer and H. J. Luger, editors, *Proceedings of the IUTAM symposium on deformation and failure of granular materials, Delft*, pages 63–68, Amsterdam, 1982. A. A. Balkema.
26. E. Azéma, F. Radjai, R. Peyroux, and G. Saussine. Force transmission in a packing of pentagonal particles. *Phys. Rev. E*, 76:011301, 2007.